Probe-Fed Linearly-Polarized Electrically-Equivalent Microstrip Antennas on FR4 Substrates

D. C. Nascimento and J. C. da S. Lacava
Laboratório de Antenas e Propagação, Instituto Tecnológico de Aeronáutica, Pr. Mal. Eduardo Gomes, 50 12228-900 São José dos Campos - SP, Brazil, {danielcn, lacava}@ita.br

***Abstract*— This paper describes a simple but efficient procedure for designing electrically-equivalent microstrip antennas on FR4 substrates. Radiation patterns, reflection coefficient magnitude (|Γ|), mutual coupling and cross-polarization level of probe-fed linearly-polarized antennas are calculated and discussed. Experimental results of |Γ| and radiation patterns of rectangular, elliptical and triangular patches validate the proposed procedure.**

***Index Terms*—** Electrically-equivalent radiators, linear polarization, low-cost substrates, microstrip antennas, new design criterion, probe-fed patches.

I. INTRODUCTION

Nowadays, one of the most widely used substrates in fabrication of conventional or multilayered printed-circuit-boards (PCBs) for fast digital circuits is the flame-retardant # 4 epoxy - or FR4 laminate [1]-[4]. This low-cost material has excellent mechanical properties [2] and consequently is a potential candidate as the substrate of printed antennas [5]-[11]. Unfortunately, the design of microstrip antennas and arrays on FR4 has not yet reached the same maturity level as those manufactured with low-loss microwave laminates [12], [13], probably because of the additional complexity added to the antenna design, namely: variations in its permittivity can shift the operating frequency whereas the high loss tangent affects the antenna bandwidth and gain, resulting in poor radiation efficiency [14].

Fortunately, this adverse scenario has recently changed with the proposal of a new efficient technique for designing low-cost probe-fed microstrip antennas [15]. Radiators can now be designed with radiation efficiency over than 70% if moderately thick substrates are used. Following this procedure, the antenna exhibits symmetrical bandwidth (with respect to the operating frequency) and real input impedance at this frequency. This technique has been applied for designing rectangular-patch antennas on FR4 substrates.

In this paper, this new technique is employed in the design of rectangular, circular and triangular microstrip antennas complying with the ISM (*Industrial, Scientific and Medical*) band. Using the electric dimension concept for antennas, three electrically-equivalent radiators are designed and analyzed. Results for radiation patterns, reflection coefficient magnitude and mutual coupling are presented and discussed.

The paper is organized as follows. A simple criterion for guiding the design of electrically-equivalent antennas, based on patch areas, is proposed in Section II. This criterion is used in Section III for

Brazilian Microwave and Optoelectronics Society-SBMO *20 Feb 2013; 28 Feb 2013; accepted 13 May 2014*
Brazilian Society of Electromagnetism-SBMag *ISSN 2179-1074*

synthesizing electrically-equivalent rectangular, elliptical and triangular antennas. Experimental results of reflection coefficient magnitude and radiation patterns validate the proposed criterion. In Sections IV and V, the mutual coupling of side-by-side and collinear array configurations are studied. Final comments are in Section VI.

II. MICROSTRIP ANTENNAS DESIGN

Using the technique introduced in [15], microstrip antennas consisting of 6.6-mm moderately thick (to obtain good radiation efficiency) FR4 substrate ($\varepsilon_r = 4.2$ and $\tan\delta = 0.02$) and square ground planes (100 mm × 100 mm), fed by 1.3-mm diameter coaxial probes, are designed at 2.45 GHz to comply with the ISM band (2.4 - 2.5 GHz). As mentioned earlier, this new technique was first applied to synthesize rectangular-patch antennas. Therefore, it is appropriate to start this chapter by designing this kind of radiator.

A. Rectangular Patch

The typical geometry of a rectangular-patch linearly-polarized (LP) microstrip antenna (with dimensions *a* and *b*) is shown in Fig. 1, where *p* denotes the probe position along the *x*-axis and *h* the substrate thickness. The antenna is directly fed by a 50-Ω SMA connector, and in order to avoid the excitation of surface waves, the patch is printed on a finite grounded dielectric layer.

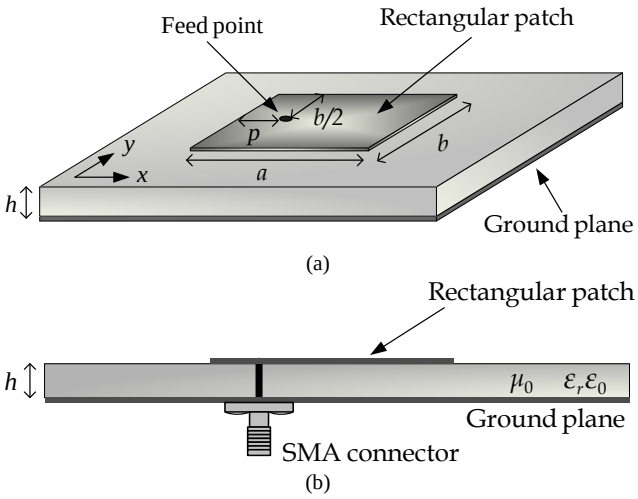

Fig. 1. Probe-fed rectangular-patch LP antenna: (a) top view - (b) side view.

Following the aforementioned procedure [15] for designing a rectangular-patch microstrip antenna in the fundamental mode TM_{10}, the operating frequency is set up at the zero input reactance condition ($X_{in} = 0$). This takes two steps; first, initial values for the patch dimensions are found using the standard approach, for example [12], [13]. Then, its feeding probe is positioned near the radiating edge ($p \cong 0$ mm). This procedure permits to check if capacitive input impedances can be reached at frequencies above the operating one. If so, it is clear that the antenna can be perfectly matched to the 50-Ω SMA connector at an intermediate position of the feeding probe, though at a frequency greater than the operating one. To carry this out, starting from the initial patch dimensions, the probe position *p* is gradually displaced from the

  ISSN 2179-1074

edge until the desired impedance is reached. The frequency where this happens must now be shifted down to the desired operating frequency through rescaling of the antenna geometry by increasing the patch dimensions *a* and *b*.

Using this procedure and the commercial software *HFSS* [16], the following optimal dimensions are obtained: a = 26.20 mm, b = 34.06 mm and p = 5.3 mm. Results for the input impedance and the reflection coefficient magnitude are shown in Figs. 2 and 3.

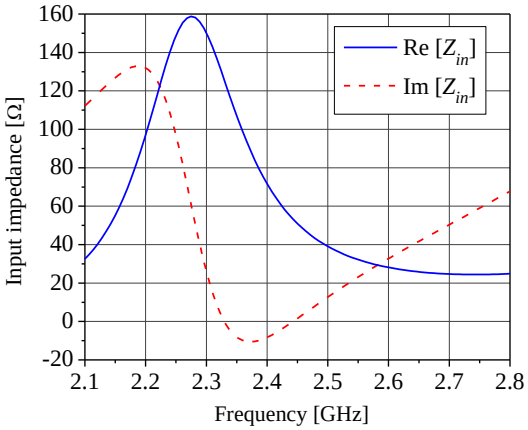

Fig. 2. Antenna input impedance.

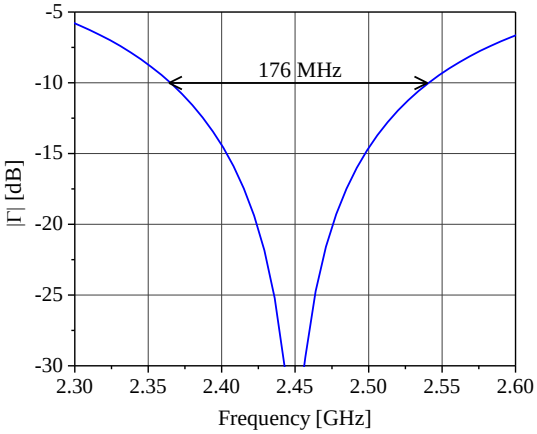

Fig. 3. Reflection coefficient magnitude.

The antenna matches perfectly the 50-Ω SMA connector and presents a 7.2 % symmetrical bandwidth (176 MHz - at 10-dB return loss condition, as shown in Fig. 3) with respect to the operating frequency (2.45 GHz), thus properly covering the ISM band. In addition, as observed in Fig. 2, the maximum resistance is greater than 50 Ω and occurs at a frequency below 2.45 GHz.

To complete the antenna analysis, radiation patterns of the E_{theta} and E_{phi} components are plotted in the *xz* and *yz* planes, as shown in Figs. 4 and 5. As noted, the *xz*-plane radiation pattern is asymmetric (Fig. 4) and the antenna cross-polarization is high, about -15 dB at $\theta = 45^{o}$ (Fig. 5). These two effects are produced by the combined action of the feeder position *p* and the moderately thick antenna substrate, in this case. Additionally, the antenna presents a radiation efficiency of 78.4 % and a directivity of 6.6 dB at the operating frequency.

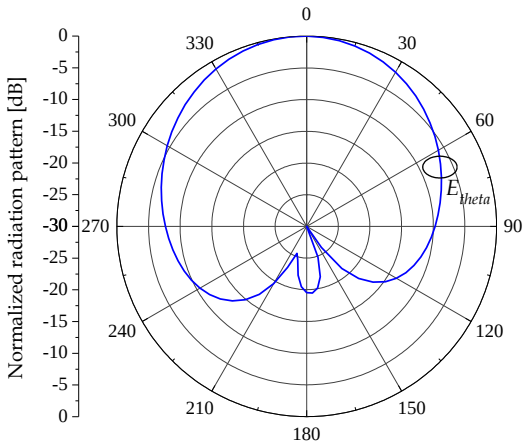

Fig. 4. Radiation pattern plotted in the *xz* plane.

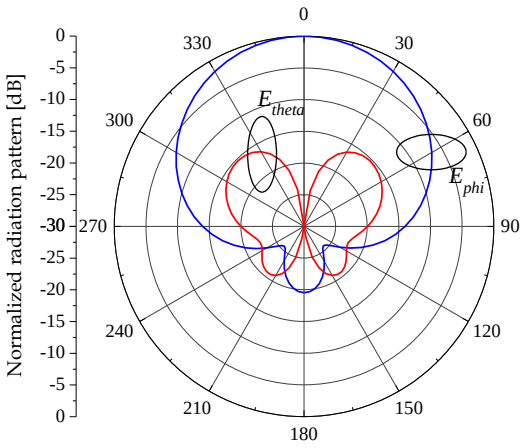

Fig. 5. Radiation pattern plotted in the *yz* plane.

20 Feb 2013; 28 Feb 2013; accepted 13 May 2014
ISSN 2179-1074

B. Circular and Triangular Patches

Using the same procedure and *HFSS* for optimizing the patch dimensions, circular and triangular patches (Figs. 6 and 7, respectively) with the same ground plane dimensions and substrate characteristics previously utilized, are also designed to operate at 2.45 GHz. The following dimensions are obtained: $2r = 31.15$ mm and $p = 9.2$ mm, for the circular patch, and $a = 35.63$ mm and $p = 3.6$ mm, for the triangular one. Figs. 8 - 10 depict the reflection coefficient magnitude and the radiation patterns. For comparison purposes, results for the rectangular-patch antenna are superimposed on these figures.

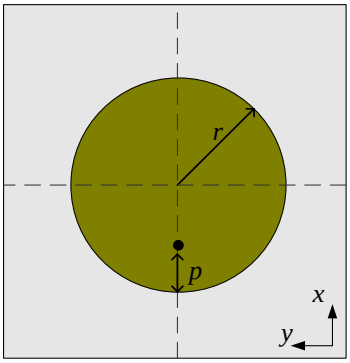

Fig. 6. Probe-fed circular-patch antenna.

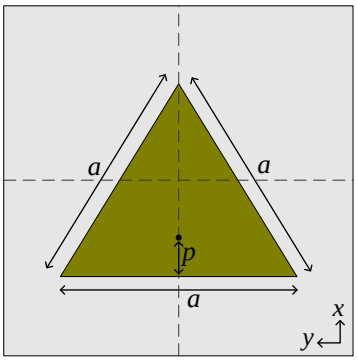

Fig. 7. Probe-fed triangular-patch antenna.

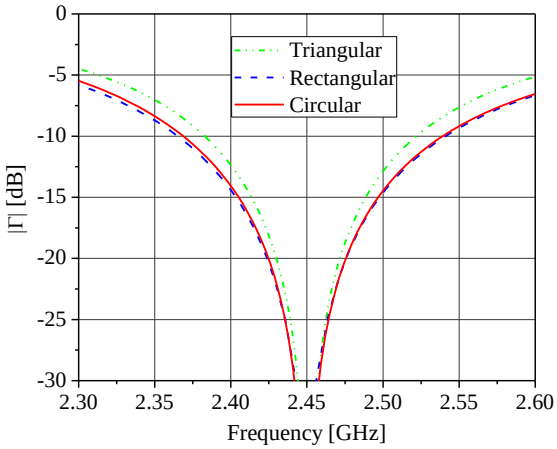

Fig. 8. Reflection coefficient magnitude.

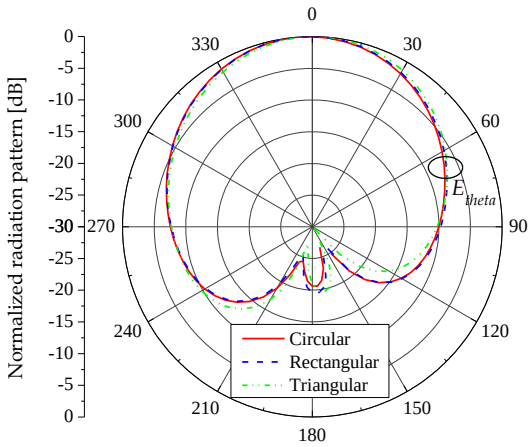

Fig. 9. Radiation pattern plotted in the *xz* plane.

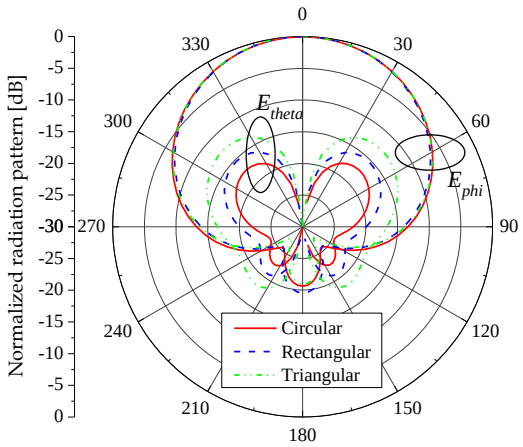

Fig. 10. Radiation pattern plotted in the *yz* plane.

20 Feb 2013; 28 Feb 2013; accepted 13 May 2014
ISSN 2179-1074

As expected, the antennas present symmetrical bandwidths with respect to the operating frequency: 6.9 % (170 MHz) for the circular patch and 5.9 % (145 MHz) for the triangular one (Fig. 8). Additionally, their radiation efficiency and directivity are: 80 % and 6.7 dB for the circular, and 76.7 % and 6.6 dB for the triangular, at the operating frequency. Therefore, the new technique permits designing three antennas perfectly matched to the 50-Ω SMA connector but with different cross-polarization (CP) levels and bandwidths: the triangular presents the higher CP level and the lowest bandwidth. However, its bandwidth (145 MHz) covers properly the ISM band (100 MHz). Thus, to design electrically-equivalent antennas (in terms of bandwidth) complying with the ISM band, it is sufficient to re-design the circular and rectangular radiators such that they exhibit the same 145-MHz bandwidth as the triangular one. But, due to the complexity of the problem, an essential question is posed at this point: which is the best way to carry out the antenna re-design?

To answer this question, it is important to remember that all antennas are designed on FR4 grounded dielectric layers with the same physical dimensions (100 mm × 100 mm; h = 6.6 mm) and for the same operating frequency (2.45 GHz). Therefore, the only physical difference among them, regardless of the geometries, is the patch area. Consequently, the electric dimensions of the antennas, on first approximation, can be considered as directly proportional to their respective patch area. As the areas are 549.7 mm^2 for the triangular patch, 762.1 mm^2 for the circular patch and 829.4 mm^2 for the rectangular patch, the triangular antenna is the electrically shortest among them, i.e., the physical area of the patch, plus the areas of the fringe fields, is smaller than those of the other antennas. Thus, to design antennas of the same bandwidth, it is sufficient to reduce the areas of the circular and the rectangular patches to a value closer to the triangular one. This procedure will be discussed next.

III. Design of Electrically-Equivalent Microstrip Antennas

Reducing the rectangular-patch area without changing the antenna operating frequency is a relatively simple task [15]. However, the same procedure can not be applied to circular patch because the antenna operating frequency is inversely proportional to its radius. Thus, an elliptical patch is considered (Fig. 11), instead of the circular one. In this case, the semi-axes of the ellipse simultaneously control the patch area and the antenna operating frequency.

Following [15] and using *HFSS* once again for optimizing the radiator dimensions, rectangular and elliptical patches, with the ground plane dimensions and substrate previously utilized, were designed to exhibit the same 5.9 %-bandwidth of the triangular-patch radiator. Starting the design procedure from the area of the triangular patch, the following dimensions are obtained: a = 32.45 mm, b = 18.8 mm and p = 11.5 mm, for the elliptical patch, and a = 26.75 mm, b = 21.45 mm and p = 8.2 mm, for the rectangular one. The areas, in the present case, are: 549.7 mm^2 for the triangular patch, 479.1 mm^2 for the elliptical patch and 573.8 mm^2 for the rectangular patch. Curves for the reflection coefficient magnitude are shown in Fig. 12. As seen, the antennas exhibit now the same 145 MHz bandwidth.

Brazilian Microwave and Optoelectronics Society-SBMO *20 Feb 2013; 28 Feb 2013; accepted 13 May 2014*
Brazilian Society of Electromagnetism-SBMag *ISSN 2179-1074*

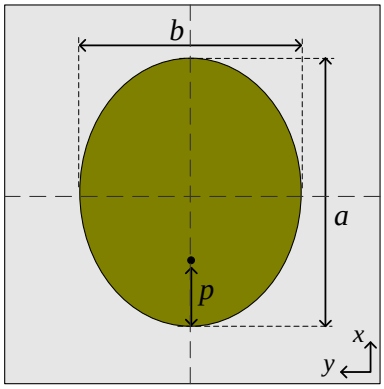

Fig. 11. Probe-fed elliptical-patch antenna.

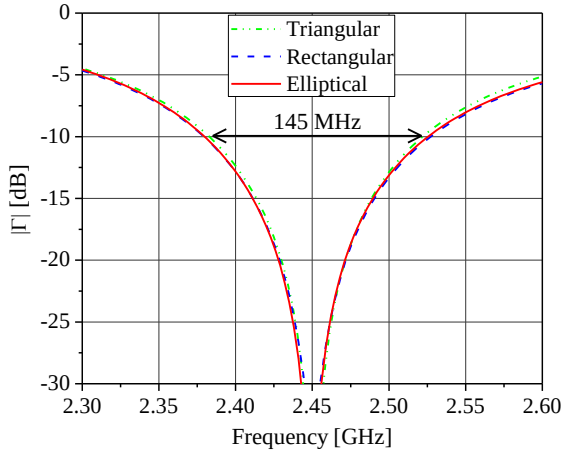

Fig. 12. Reflection coefficient magnitude.

Radiation patterns in the *xz* and *yz* planes are shown in Figs. 13 and 14, respectively. Since there is no substantial difference between the co-polarized patterns, and the curves of the reflection coefficient magnitudes are substantially coincident, it can be stated that the new procedure permits the design of three electrically-equivalent radiators. However, it is important to point out the different behavior, in the *xz*-plane (E_{theta} component), of the cross-polarization of the triangular-patch antenna.

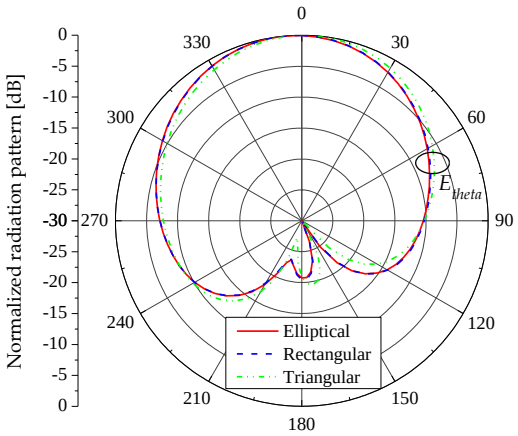

Fig. 13. Radiation pattern plotted in the *xz* plane.

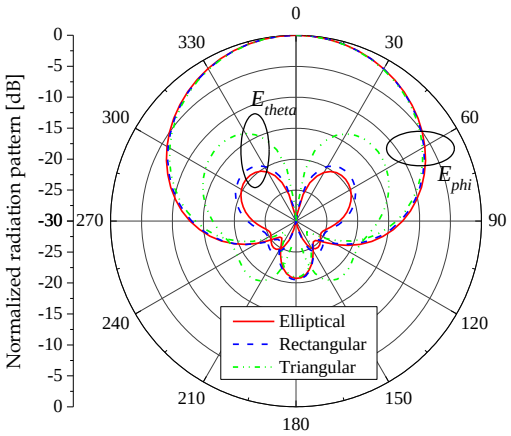

Fig. 14. Radiation pattern plotted in the *yz* plane.

Additional comparisons presented in Table I show that the radiation efficiency and directivity of the three antennas are similar. The directivity equivalence was expected, in view of the similarity among the antenna radiation patterns. However, the cross-polarization level is more discrepant, as mentioned.

TABLE I. ELECTRIC CHARACTERISTICS OF LP MICROSTRIP ANTENNAS

	Rectangular	**Elliptical**	**Triangular**
Directivity	6.62 dB	6.56 dB	6.60 dB
Radiation Efficiency	78.4 %	77.2 %	76.7 %
Cross-polarization	-18.6 dB (θ = 50°)	-19.5 dB (θ = 50°)	-12.6 dB (θ = 45°)

Prototypes were built to validate the simulated results. The patches are positioned at the center of the square (100 mm × 100 mm) grounded FR4 dielectric, according to the geometries presented in Figs. 1, 7 and 11. Photos of the prototypes are shown in Figs. 15 - 17. Simulated and measured results for the reflection coefficient magnitude are shown in Fig. 18. As seen, the experimental data are in complete agreement among themselves, although 22.5 MHz down from the simulated results. This is because of the inaccuracy of the FR4 permittivity, as mentioned in [14]. As we have confidence in the simulation procedure and in the manufacturing process, any difference between simulation and experimental data can be attributed to the variation in the substrate dielectric permittivity. Thus, instead of the nominal 4.2, the relative permittivity of the FR4 laminate we used is actually around 4.29.

Fig. 15. Rectangular-patch prototype.

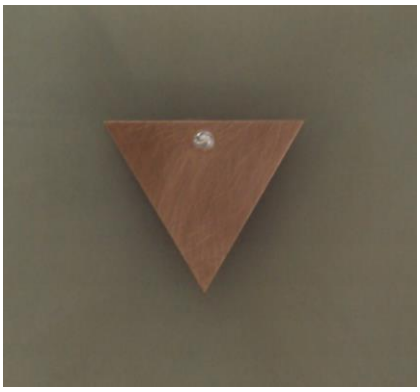

Fig. 16. Triangular-patch prototype.

Fig. 17. Elliptical-patch prototype.

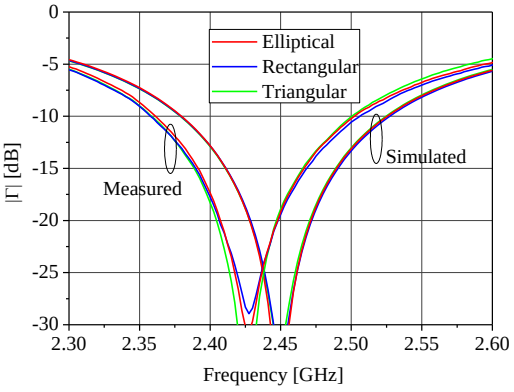

Fig. 18. Reflection coefficient magnitude: simulated and measured.

ISSN 2179-1074

Radiation patterns in the *yz* plane, measured in the IF-DCTA anecoic chamber, are shown in Figs. 19-21. As seen, very good agreements with simulated results are obtained, validating the design procedure. The differences derive from the lack of a *balun* in the coaxial feed line.

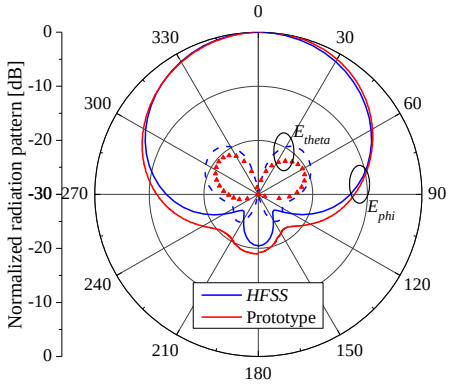

Fig. 19. Radiation patterns in the *yz* plane: rectangular patch.

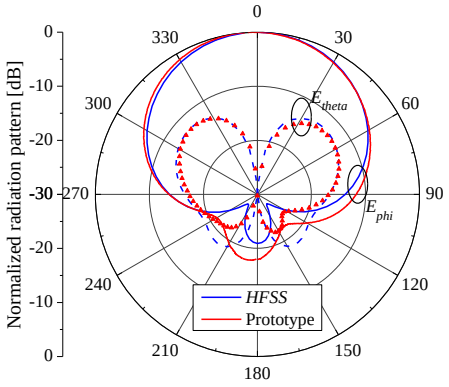

Fig. 20. Radiation patterns in the *yz* plane: triangular patch.

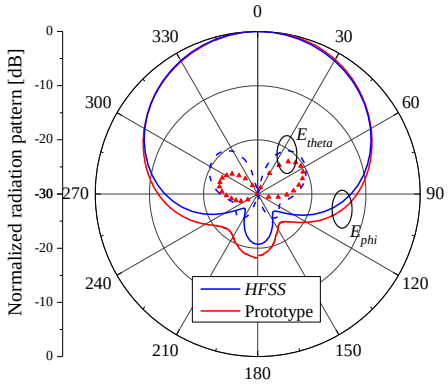

Fig. 21. Radiation patterns in the *yz* plane: elliptical patch.

IV. Mutual Coupling Between Antennas of Equal Patches

Mutual coupling is an important effect related to array design. For the specific case of microstrip arrays, mutual couplings, as well as the radiation patterns, are dependent on the thickness and the electric characteristics of the substrate, the grounded dielectric dimensions, the patch displacement and their relative position. Arrays made out of two patches of equal geometries, such as rectangular, elliptical or triangular, both designed for the same bandwidth (145 MHz), were simulated in *HFSS* for a fixed $\lambda_0/2$ displacement *d* between their geometric centers. In the first arrangement, denoted by *A*, the elements are in the classical side-by-side configuration, i.e., the main current distributions are positioned according to Fig. 22. In the second, named *B*, they are in the collinear configuration, as shown in Fig. 23.

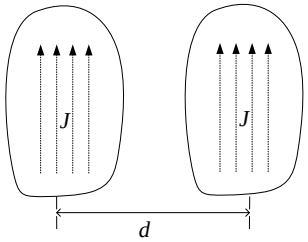

Fig. 22 Side-by-side configuration.

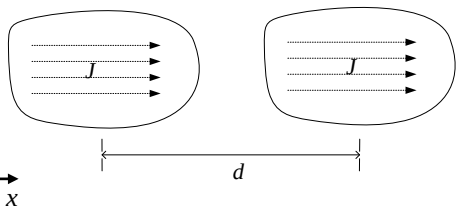

Fig. 23. Collinear configuration.

20 Feb 2013; 28 Feb 2013; accepted 13 May 2014
ISSN 2179-1074

Simulations are performed for the geometries established in Section III, all positioned in the center of a rectangular (160 mm × 100 mm) grounded FR4 layer. Table II shows the level of the mutual coupling of six different arrays, simulated at 2.45 GHz. The letters *A* and *B* indicate the array topology (side-by-side or collinear) and the index specifies the elements of the array - *E* designates the elliptical patch, *R* the rectangular and *T* the triangular one.

TABLE II. MUTUAL COUPLING BETWEEN MICROSTRIP ANTENNAS OF EQUAL PATCHES

Configuration	$\|S_{21}\|$ dB	Configuration	$\|S_{21}\|$ dB
A_E	-19,0	B_E	-19,6
A_R	-18,7	B_R	-19,5
A_T	-18,8	B_T	-20,1

It can be seen from these results that the level of the mutual coupling is almost independent of the patch geometry, since the radiators, in this case, are designed to have the same bandwidth (according to the criterion proposed in this work). Thus, for arrays of type *A*, the mutual coupling is close to -19 dB, with a maximum variation of 0.3 dB. On the other hand, arrays of type *B* present mutual coupling of about -20 dB, with variation of 0.6 dB. Note that the best value for mutual coupling is obtained for the B_T configuration, i.e., the collinear array of triangular patches.

Broadside radiation patterns in the *yz* and *xz* planes are shown in Figs. 24 and 25 for side-by-side and collinear configurations, respectively. As the antennas are electrically equivalent, similar broadside radiation patterns are obtained. However, the side-by-side configuration presents a back lobe greater than the collinear one. This lobe occurs because the edge diffraction of the electric field co-polarized component in the side-by-side configuration is more intense than the same polarization in the collinear one. Moreover, the side-by-side configuration is slightly more directive (9.2 dB) than the collinear one (8.9 dB). It can also be noted that the arrays' cross-polarization is better than -30 dB.

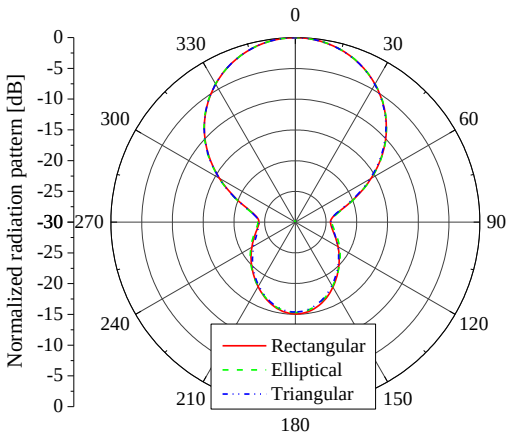

Fig. 24. Side-by-side radiation pattern: *yz* plane.

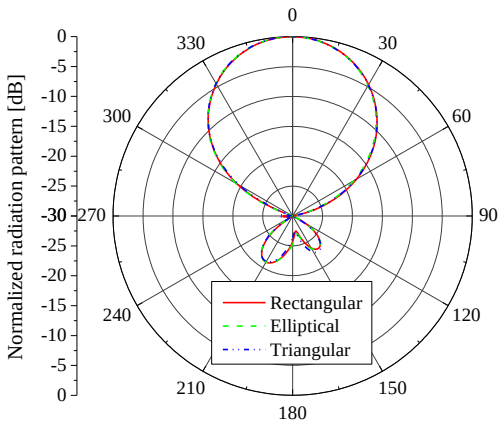

Fig. 25. Collinear radiation pattern: *xz* plane.

ISSN 2179-1074

V. MUTUAL COUPLING BETWEEN ANTENNAS OF DIFFERENT PATCHES

The criterion introduced in Section III for designing microstrip antennas results in electrically-equivalent elements, i.e., radiators that have substantially equivalent radiation patterns, directivities and radiation efficiencies. This leads to the possibility of fabricating microstrip arrays of different patch geometries, but the same bandwidth.

This section is therefore devoted to the study of particular cases, focusing on configurations with the lowest mutual couplings. As in the previous section, the relative displacement d is fixed as $\lambda_0/2$ and the simulations are performed at 2.45 GHz for two different arrangements - where again the letter A indicates the side-by-side configuration and B the collinear one - with the patches positioned in the center of the rectangular (160 mm × 100 mm) grounded FR4 layer. Fig. 26 shows a side-by-side array composed by rectangular and triangular elements, i.e., the array denoted by A_{RT}.

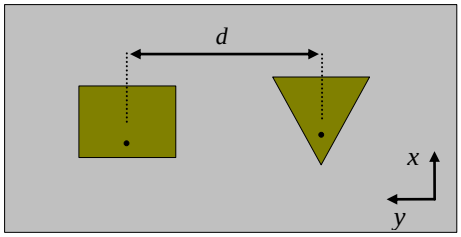

Fig. 26. Side-by-side A_{RT} configuration.

A third index is employed for the configuration B in order to specify the feeding probe position. The index 2 is used in cases the coaxial probes are farther apart. To illustrate, Fig. 27 shows the B_{ET} configuration whereas the B_{ET2} is represented in Fig. 28. Table III shows the mutual coupling results for ten different array configurations.

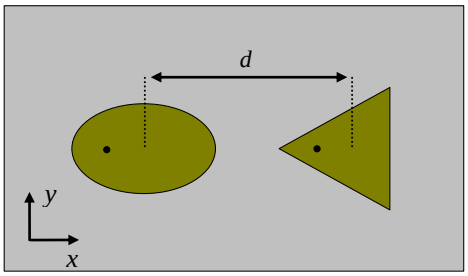

Fig. 27. Collinear B_{ET} configuration.

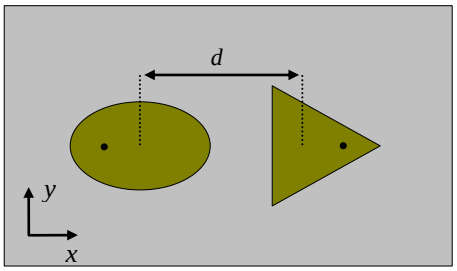

Fig. 28. Collinear B_{ET2} configuration.

TABELA III. MUTUAL COUPLING BETWEEN MICROSTRIP ANTENNAS OF DIFFERENT PATCHES

Configuration	$\|S_{21}\|$ dB	Configuration	$\|S_{21}\|$ dB
$\boldsymbol{A_{ER}}$	-18.8	$\boldsymbol{B_{RT}}$	-19.4
$\boldsymbol{A_{ET}}$	-18.9	$\boldsymbol{B_{RT2}}$	-23.8
$\boldsymbol{A_{RT}}$	-18.8	$\boldsymbol{B_{ET2}}$	-23.9
$\boldsymbol{B_{ER}}$	-19.4	$\boldsymbol{B_{RR2}}$	-22.8
$\boldsymbol{B_{ET}}$	-19.9	$\boldsymbol{B_{TT2}}$	-24.7

ISSN 2179-1074

As in previous cases (Table II), the mutual coupling is almost independent of the patch geometries, being more dependent on the array configurations. For side-by-side arrays the mutual coupling ranges from -18.8 dB to -18.9 dB. On the other hand, for collinear B_{ER}, B_{ET} and B_{RT} array configurations, the range is from -19.4 dB to -19.9 dB. Finally, for the index 2 configurations, the mutual coupling range is from -22.8 dB to -24.7 dB. This latter configuration is not very common but has been used in order to minimize the cross-polarization level of linear arrays [17].

Broadside radiation patterns in the *yz* and *xz* planes are shown in Figs. 29 and 30 for side-by-side and collinear (not index 2) configurations, respectively. For comparison purposes, radiation patterns calculated in the last section for the rectangular-patch array are superimposed on these figures. Once again, as the antennas are electrically equivalent, similar broadside radiation patterns are obtained.

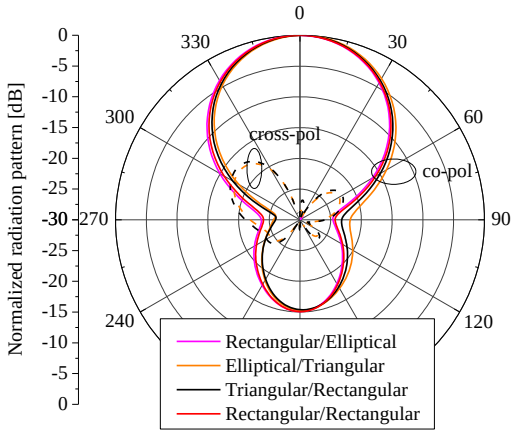

Fig. 29. Side-by-side radiation pattern: *yz* plane.

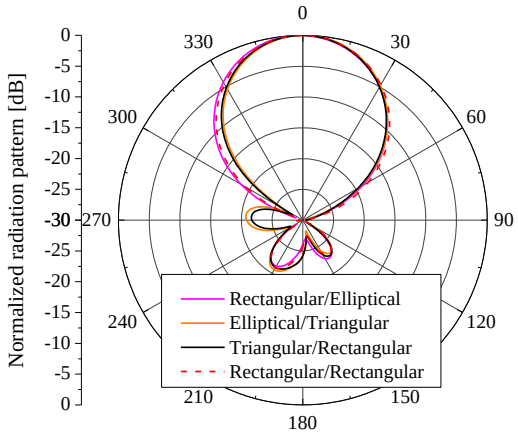

Fig. 30. Collinear (without index 2) radiation pattern: *xz* plane.

However, strong cross-polarization content appears in the *yz*-radiation plane of the side-by-side configuration with triangular patches. This results from the great difference between the current patterns for the resonance modes of each array element [12], even when designed to be electrically equivalent.

VI. Final Comments

In this paper, a comprehensive study of probe-fed linearly-polarized electrically-equivalents microstrip antennas on FR4 substrates, synthesized according to the zero input reactance condition, was presented. In this innovative technique, introduced in [15] for designing moderately thick antennas, judicious choices for the patch dimensions and probe position can compensate for the probe reactance, without the need for any external matching network, which would increase the complexity of the antenna analysis and construction. This technique was used for designing antennas with rectangular, circular and triangular patches, in the ISM band (2.4 - 2.5 MHz), resulting in three antennas perfectly matched to the 50-Ω SMA connector but with different cross-polarization levels and bandwidths: the triangular patch antenna presented the highest CP level and the lowest bandwidth. These behaviors indicated the need to develop a simple but

  ISSN 2179-1074

efficient new strategy for designing electrically equivalent antennas, whatever the patch geometry. Using this new strategy, based on the electric dimensions of the antennas (on first approximation, considered directly proportional to the patch area), antennas with a rectangular, elliptical and triangular patch were synthesized for equivalent performance, in terms of bandwidth. Consequently, their radiation patterns, directivity and radiation efficiency were also shown to be substantially equivalent. Upon applying this criterion, the mutual coupling between microstrip antennas was analyzed. It was shown that the mutual coupling level, in case of probe-fed low-cost radiators, is equivalent, whatever the patch geometry. Similar results were obtained for the radiation characteristics of broadside arrays in both side-by-side and collinear configurations.

Although the present procedure had been formulated for low-cost antennas, it is general and can be applied for designing antennas on low-loss moderately thick laminates with different feeding techniques.

ACKNOWLEDGMENT

The authors would like to thank CNPq for sponsoring project no. 402017/2013-7, to IFI-DCTA for providing the use of the anechoic chamber and Eng. Nilson Rabelo for the assistance in preparation of the manuscript.

REFERENCES

[1] J. R. Aguilar, M. Beadle, P. T. Thompson, and M. W. Shelley, "The microwave and RF characteristics of FR4 substrates," *IEE Low-Cost Antenna Technol. Colloq.* London, UK, vol. 24, pp. 2/1-2/6, Feb. 1998.

[2] A. R. Djordjevic, R. M. Biljic, V. D. Likar-Smiljanic, and T. K. Sarkar, "Wideband frequency-domain characterization of FR-4 and time-domain causality," *IEEE Trans. Electromagn. Compat.*, vol. 43, no. 4, pp. 662-667, Nov. 2001.

[3] E. L. Holzman, "Wideband measurements of the dielectric constant of an FR4 substrate using a parallel-coupled microstrip resonator," *IEEE Trans. Microwave Theory Tech.*, vol. 54, no. 7, pp. 3127-3130, July 2006.

[4] J. C. Rautio and S. Arvas, "Measurement of planar substrate uniaxial anisotropy," *IEEE Trans. Microwave Theory Tech.*, vol. 57, no. 10, pp. 2456-2463, Oct. 2009.

[5] M. Amman, "A comparison of some low cost laminates for antennas operating in the 2.45 GHz ISM band," *IEE Low-Cost Antenna Technol. Colloq.* London, UK, vol. 24, pp. 3/1-3/5, 1998.

[6] R. Lelaratne and R. J. Langley, "Dual-band patch antenna for mobile satellite systems," *IEE Proc.-Microw. Antennas Propag*., vol. 173, no 6, pp. 427-430, Dec. 2000.

[7] R. Gardelli, G. La Cono, and M. Albani, "A low-cost suspended patch antenna for WLAN access points and point-to-point links," *IEEE Antennas and Wireless Propagation Letters*, vol. 3, pp. 90-93, 2004.

[8] M. Niroojazi and M. N. Azarmanesh, "Practical design of single feed truncated corner microstrip antenna," *Proc. Second Annual Conference on Communication Networks and Services Research*, Fredericton, NB, Canada, pp. 25-29, May 2004.

[9] D. Bhardwa an D. Bhatnagar, "Radiation from double notched square patch antenna on FR4 substrate," *Journal of Microwaves, Optoelectronics and Electromagnetic Applications*, vol. 7, no. 2, pp. 54-64, Dec. 2008.

[10] G. Immadi, M. S. R. S. Tejaswi, M. V. Narayama, N. A. Babu, G. Anupama, and K. V. Raviteja, "Design of coaxial fed microstrip patch antenna for 2.4 GHz BLUETOOTH applications," *Journal of Emerging Trends in Computing and Information Sciences*, vol. 2, no. 12, pp, 686-690, Dec. 2011.

[11] A. A. Qureshi, M. U. Afzal, T. Taqueer, and M. A. Tarar, "Performance analysis of FR-4 substrate for high frequency microstrip antennas," *Proc. China-Japan Joint Microwave Conferece*, Hangzhou, pp. 01-04, Apr. 2011.

[12] R. Garg, et al., *Microstrip Antenna Design Handbook*, Norwood, MA, Artech House, 2001.

[13] J. L. Volakis (editor), *Antenna Engineering Handbook*, Fourth Edition, New York, McGraw-Hill, 2007.

[14] D. C. Nascimento, "Antennas for mobile communications," *M.Sc. Thesis*, Technological Institute of Aeronautics, São José dos Campos, Brazil, 2007 (in Portuguese).

[15] D. C. Nascimento and J. C. S. Lacava, "Design of low-cost probe-fed microstrip antennas," In: *Microstrip Antennas*, Nasimuddin (Ed.), InTech, Chapter 01, pp. 01-26, 2011.

[16] HFSS (2012), Product overview, *Available http://www.ansys.com/Products/Simulation+Technology/Electromagnetics/High-Performance+Electronic+Design/ANSYS+HFSS* (Oct. 2012).

[17] L. F. Marzall, R. Shildberg, and J. C. S. Lacava, High-performance, low-cross-polarization suspended patch array for WLAN applications. *Proc. Antennas and Propag. Society Int. Symp*., Charleston, SC, USA, July 2009.

